Articles

New Commensurate Phases in the Family (A$_3$Co$_2$O$_6$)$_\alpha$(A$_3$Co$_3$O$_9$)$_\beta$ (A = Ca, Sr, Ba)

K. Boulahya, M. Parras, and J. M. González-Calbet*

Departamento de Química Inorgánica, Facultad de Químicas, Universidad Complutense, 28040-Madrid, Spain

New phases with one-dimensional structures in the A−Co−O system (A = Ca, Sr, Ba) have been isolated and characterized by electron diffraction and high-resolution electron microscopy. (Ca$_{0.4}$Sr$_{0.6}$)$_9$Co$_7$O$_{21}$, Sr$_{14}$Co$_{11}$O$_{33}$, Sr$_{21}$Co$_{17}$O$_{51}$, Ba$_{15}$Co$_{13}$O$_{39}$, and Ba$_{66}$Co$_{59}$O$_{177}$ are members of an homologous series of general formula (A$_3$Co$_2$O$_6$)$_\alpha$(A$_3$Co$_3$O$_9$)$_\beta$. All of them are constituted by the ordered intergrowth of structural frames of the phases limiting this series: Ca$_3$Co$_2$O$_6$ and 2H−BaCoO$_3$. All of the members of this series are commensurate phases derived by a modulation vector $\mathbf{k} = (a^*_{2H} + b^*_{2H})/3 + m2c^*_{2H}$, with m being related to the numbers α and β and, consequently, giving directly the A/Co ratio. The ordered succession of blocks can unambiguously be obtained from the HREM images.

Introduction

Inorganic structures with one-dimensional atomic arrangements are in the limelight because of unique physical properties. One of the structural types most studied in the past decade refers to a particular kind of AB$_{1−x}$O$_{3−3x}$ ($x \leq 1$) hexagonal perovskite-type compounds. The structures of these materials are built up from infinite BO$_3$ chains consisting of alternating octahedral and trigonal prismatic units separated by A cations. Their structural relationships with the 2H-ABO$_3$[1]-related perovskite have been previously reported.[2,3]

Between Ca$_3$Co$_2$O$_6$, which is made up of polyhedra chains formed by the alternation of an octahedron linked by common faces to a trigonal prism (TP) both occupied by Co atoms,[4] and 2H−BaCoO$_3$,[5] which is only built up of [BO$_6$] octahedra (O$_h$) sharing faces running parallel to the *c* axis, several materials have been stabilized with the general composition A$_{n+2}$A′B$_n$O$_{3n+3}$[6] (with A′ and B corresponding to cations in prismatic and octahedral coordination, respectively). All of these phases can be described in terms of a hexagonal stacking of mixed A$_3$O$_9$ and A$_3$A′O$_6$ layers.[2] Besides $n = 1$ (Ca$_3$Co$_2$O$_6$) and ∞ (2H−BaCoO$_3$), the members $n = 2−7$ have been

reported for A′ = B≡Co, the A positions being occupied by Ca, Sr, or Ba.[6,7] All of these phases show structures with one TP per unit formula, n indicating the number of octahedra between TP. However, with the A$_{n+2}$-A′B$_n$O$_{3n+3}$ formulation, the structures existing outside of these rules cannot be easily described. For instance, in Ba$_{14}$Cu$_3$Ir$_8$O$_{33}$, Ba$_{16}$Cu$_3$Ir$_{10}$O$_{39}$, and Ba$_9$Cu$_2$Ir$_5$O$_{21}$, recently reported by Blake et al.,[8] more than 1 TP per unit formula exists, because they can be considered as the ordered intergrowth of different members of the above series. As a consequence, the number of octahedra between trigonal prisms is not constant. In such series, the above-mentioned materials should correspond to members with fractional values of n, such as $n = 2.67$ (...TP:2O$_h$:TP:3O$_h$:TP:3O$_h$...), $n = 3.33$ (...TP:3O$_h$:TP:3O$_h$:TP:4O$_h$...), and $n = 2.5$ (...TP:2O$_h$:TP:3O$_h$...). According to these ideas, the authors propose a classification scheme considering that the structures can be described as composites containing two substructures with the same unit cell parameters a and b but with different c_1 and c_2 parameters, as previously reported by Ukei et al.[9] Here, c_1 is associated with the columns of A cations and c_2 with the atoms in polyhedra. The unit cell is commensurate when $pc_1 = qc_2$ and incommensurate when c_1/c_2 is not a rational fraction, with $2p$ being the number of layers, either A$_3$O$_9$ or A$_3$A′O$_6$, and q as the number of polyhedra per unit cell.

* To whom correspondence should be addressed. Telephone: 34 91 394 43 42. Fax: 34 91 394 43 52. E-mail: jgcalbet@eucmax.sim.ucm.es.
(1) Lander J. J. *Acta Crystallogr.* **1951**, *4*, 148.
(2) Darriet, J.; Subramanian, M. A. *J. Mater. Chem.* **1995**, *5*, 543.
(3) Dussarrat, C.; Grasset, F.; Darriet, J. *Eur. J. Solid State Inorg. Chem.* **1995**, *32*, 557.
(4) Fjellvag, H.; Gulbrandsen, E.; Aasland, S.; Olsen, A.; Hauback, B. C. *J. Solid State Chem.* **1996**, *124*, 190.
(5) Taguchi, H.; Takeda, Y.; Kanamara, F.; Shimada, M.; Kaizomi, M. *Acta Crystallogr. B* **1977**, *33*, 1299.
(6) Boulahya, K.; Parras, M.; González-Calbet, J. M. *J. Solid State Chem.* **1999**, *142*, 419.

(7) Boulahya, K.; Parras, M.; González-Calbet, J. M. *J. Solid State Chem.* **1999**, *145*, 116.
(8) Blake, G. R.; Sloan, J.; Vente, J. F.; Battle, P. D. *Chem. Mater.* **1998**, *10*, 3536.
(9) Ukei, A.; Yamamoto, A.; Watanabe, Y.; Shishido, T.; Fukuda, T. *Acta Crystallogr. B* **1993**, *49*, 67.
(10) Evain, M.; Boucher, F.; Gourdon, O.; Petricek, V.; Dusek, M.; Berdicka, P. *Chem. Mater.* **1998**, *10*, 3068.

Evain et al.[10] have reported a new structure determination on a single crystal of the $Sr_{1.2872}NiO_3$ incommensurate composite hexagonal compound. They describe the hexagonal perovskite structure as a composite structure with two chain subsystems: an $[(A',B)X_3]$ first-chain subsystem and an $[A]$ second-chain subsystem. With $\mathbf{q} = \gamma c_s{}^*$ as the modulation wave vector, the most instructive formula can be established is $(A_2A'X_3)_{2\gamma-1}$-$(ABX_3)_{2(1-\gamma)}$. Considering that $O_h/TP = 2(1 - \gamma)/(2\gamma - 1)$, the stoichiometry and the O_h/TP relationship can be directly obtained from the diffraction pattern. In the case of a commensurate composite structure, the γ component of the $\mathbf{q}$ vector can be expressed as a rational fraction, $\gamma = m/n$, with $2m$ being the number of A cations per formula and n the number of polyhedra per row. Notice that m is equal to p and n corresponds to m in the Blake et al. notation.[8]

We describe in this paper new phases in the A–Co–O system (A = Ba, Sr, Ca) formed, as confirmed by high-resolution electron microscopy (HREM), by the ordered intergrowth of integer members of the $A_{n+2}A'B_nO_{3n+3}$ series. By considering the structural blocks constituting these materials as a new formulation, $(A_3B_2O_6)_\alpha$-$(A_3B_3O_9)_\beta$, is proposed, which allows us to account for all compounds. The study by selected area electron diffraction (SAED) indicates that all powdered samples are commensurate with a modulation vector $\mathbf{k} = (a^*{}_{2H} + b^*{}_{2H})/3 + m2c^*{}_{2H}$. The z component of this vector is related to the composition and the number of each block constituting the unit cell. This formulation agrees with that proposed by Evain et al.,[10] suggesting that at least the essential features of these compounds can be characterized even when single crystals are not available.

Experimental Section

Several preparative strategies can be adopted to isolate new phases. The simplest consists of preparing equimolar ratios between consecutive members of the family. Thus, the combination between $n = 2$ and 3-members should lead to the (9:7) phase according to $1A_4B_3O_9{:}1A_5B_4O_{12} = A_9B_7O_{21}$. Besides, by taking into account that the c axis in odd members is double with respect to that corresponding to even members, another possibility should consist in preparing the ordered intergrowth between unit cells of consecutive members. For $n = 2$ and 3, the stoichiometric ratio should be $1A_4B_3O_9{:}2A_5B_4O_{12} = A_{14}B_{11}O_{33}$. Both compositions would require fractional values of n, $^5/_2$ and $^8/_3$, respectively, in the above family.

If we keep B=Co the same, the synthesis strategy requires the adequate selection of both size A cation and annealing temperature and time. Materials have been prepared by heating in air stoichiometric amounts of ACO_3 (A = Ca, Sr, Ba) and Co_3O_4 according to the temperature and annealing times shown in Table 1. Black products are obtained in all cases.

The average cationic composition was established by inductive-coupling plasma. The local composition in every crystal was determined by energy dispersive spectroscopy (EDS) on a JEOL scanning electron microscope JSM-8600 equipped with an energy-dispersive system LINK AN10000. All results are consistent with the nominal compositions. The oxygen content was determined, within $\pm 1 \times 10^{-2}$, from the average oxidation state of cobalt analyzed by titration using Mohr's salt. The Co average oxidation state is, in all cases, very close to $[4z - 2(x - z)]/z$, with x and z being the number of Ba and Co atoms, respectively, per unit formula.

Powder X-ray diffraction was performed on a Philips X'Pert diffractometer using Cu Kα radiation. Unit cell parameters of the isolated single phases are also listed in Table 1.

SAED was carried out on a JEOL 2000FX electron microscope, fitted with a double-tilting goniometer stage ($\pm 45°$). HREM was carried out on a JEOL 4000EX electron microscope, fitted with a double-tilting goniometer stage ($\pm 25°$), by working at 400 Kv. Samples were dispersed in *n*-butanol and transferred to carbon-coated copper grids. Simulated HREM images were calculated using the Mac Tempas program.

Results

1. (Sr, Ca)–Co–O system. Figure 1a shows the SAED pattern along $[1\bar{1}00]_{2H}//[\bar{1}010]_{9:7}$ corresponding to $(Sr_{0.6}Ca_{0.4})_9Co_7O_{21}$. A 9-fold modulated superstructure can be observed following the $[33\bar{6}4]^*{}_{2H}$ direction. It is worth emphasizing that the modulation direction is always perpendicular to the planes containing Co atoms in TP.[7] The corresponding HREM image (Figure 1b) shows an apparently well-ordered material, whose structure can be described as an ordered intergrowth between a (4:3) unit cell and half of a unit cell of the (5:4) phase. Therefore, the unit cell is constituted by 18 layers (6 A_3O_9 and 12 A_3BO_6) as due to the following sequence of polyhedra: ...1TP:2O_h:1TP:3O_h.... Figure 1c shows the corresponding structural model along $[1\bar{1}00]_{2H}$ that constitutes the $n = 2.5$-member of the A_{n+2}-$CoCo_nO_{3n+3}$ homologous series, with parameters $a = 0.93$ nm and $c = 3.63$ nm, rhombohedral symmetry and space group $R\bar{3}c$. This phase is isostructural to Sr_9-Ni_7O_{21}.[11,12] According to the corresponding atomic coordinates and by considering a random distribution of Sr and Ca atoms, an image calculation has been performed (Figure 1). The best fit is obtained for $\Delta t = 7.5$ nm and $\Delta f = -95$ nm.

Figure 2a shows the SAED pattern along $[1\bar{1}00]_{2H}//[\bar{1}010]_{14:11}$ corresponding to $Sr_{14}Co_{11}O_{33}$. The structural features are similar to those previously shown.[8] Now, the modulation direction, perpendicular to the planes containing Co atoms in trigonal prisms, is $[14\ 14\ i\ 18]^*{}_{2H}$, intermediate between $[44\bar{8}6]^*{}_{2H}$, as in the (4:3) phase, and $[55i6]^*{}_{2H}$, as in the (5:4) phase. Following this direction, all satellite reflections are equidistant, with their intensity decreasing as the order of the reflections increases. Only sixth-order satellites are seen and, as a consequence, SAED patterns showing such characteristics have been erroneously interpreted by other authors as due to incommensurate phases.[13] However, the corresponding HREM image (Figure 2b) shows an apparently well-ordered material, whose structure is formed by the ordered intergrowth of a (5:4) unit cell with another unit cell corresponding to the (4:3) phase. Therefore, the unit cell corresponding to $Sr_{14}Co_{11}O_{33}$ is formed by 14 layers (5 A_3O_9 and 9 A_3-BO_6), leading to isolated rows of polyhedra sharing faces, according to the sequence ...1TP:2O_h:1TP:3O_h:1TP:3O_h.... The structural ideal model, projected along $[1\bar{1}00]_{2H}$ is shown in Figure 2c. From the corresponding atomic coordinates, an image calculation has been performed. The best fit is obtained for $\Delta t = 7.0$ nm and $\Delta f = -90$ nm (Figure 2). Once again, because there are more than one prisms per row per unit cell, this material

(11) Campá, J.; Gutierrez-Puebla, E.; Monge, A.; Rasines, I.; Ruiz-Valero, C. *J. Solid State Chem.* **1996**, *126*, 27.

(12) Huvé, M.; Renard, C.; Abraham, F.; Van Tendeloo, G.; Amelinckx, S. *J. Solid State Chem.* **1998**, *135*, 1.

(13) Battle, P. D.; Blake, G. R.; Sloan, J.; Vente, J. F. *J. Solid State Chem.* **1998**, *136*, 103.
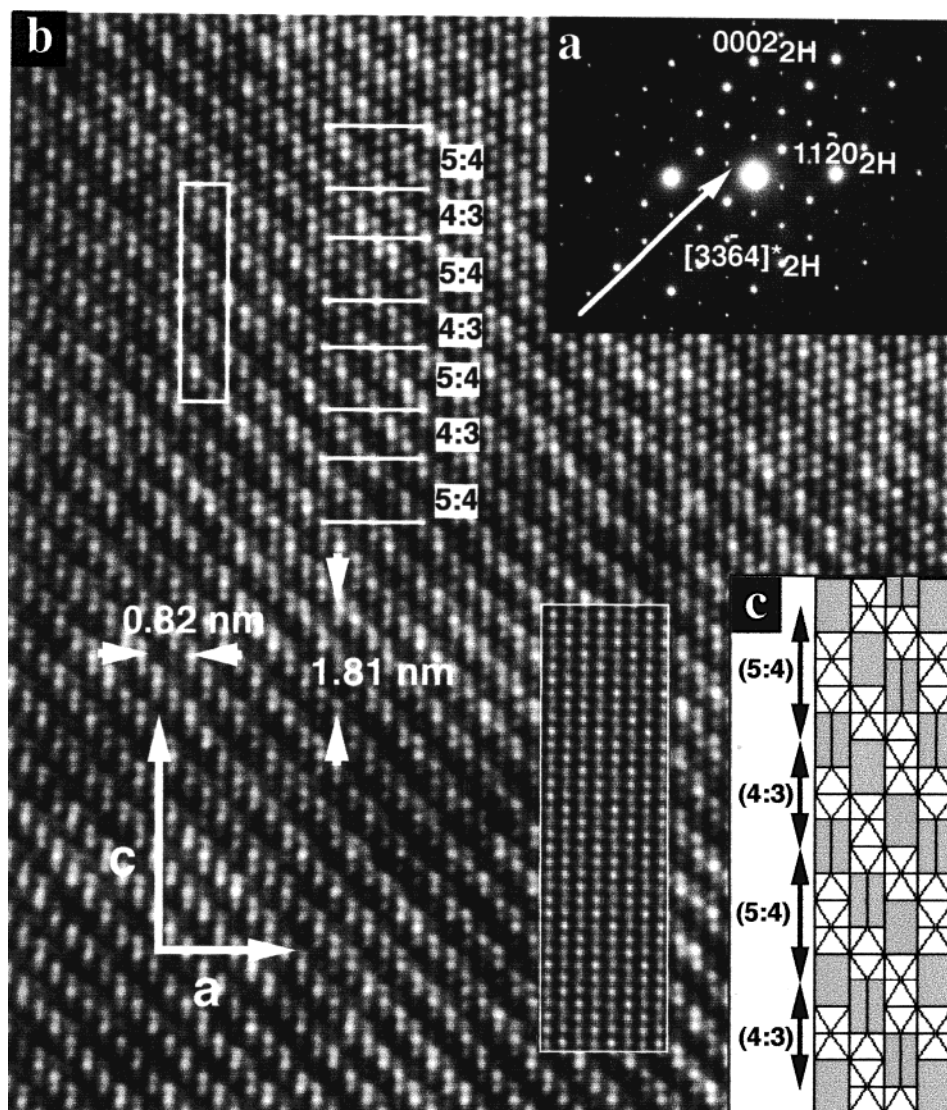
Figure 1. (a) SAED pattern along $[1\bar{1}00]_{2H}$ corresponding to $(Ca_{0.4}Sr_{0.6})_9Co_7O_{21}$. The 2H modulation direction is marked with an arrow. (b) Corresponding HREM image. The simulated image is shown at the inset. (c) Ideal structural model along $[1\bar{1}00]_{2H}$, formed by the ordered intergrowth of one (5:4) and one (4:3) blocks along c axis.

does not constitute an integer member of the homologous series but can be considered as the $n = 2.66$ member of the family. Unit cell parameters are $a = 0.94$ nm and $c = 2.86$ nm, with trigonal symmetry and space group $P321$.

Between $n = 3$ and 4, another ordered material has been isolated according to the ratio $3Sr_5Co_4O_{12}:1Sr_6Co_5O_{15}$. This is the $Sr_{21}Co_{17}O_{51}$ phase that would correspond to the $^{13}/_4$ member of the $A_{n+2}CoCo_nO_{3n+3}$ family. Figure 3a shows the corresponding SAED pattern along $[1\bar{1}00]_{2H}//[10\bar{1}0]_{21:17}$. The modulation direction is, in this case, $[2121i24]^*_{2H}$, up to third-order satellites being observed. The corresponding HREM (Figure 3b) shows again an apparently ordered material due to the intergrowth between one and a half unit cell of the (5:4) phase with one unit cell of the (6:5). The new unit cell is formed by 42 layers (18 Sr_3O_9 and 24 Sr_3CoO_6) with trigonal symmetry and unit cell parameters $a = 0.94$ and $c = 8.49$ nm, constituting the $n = 3.25$ member of the homologous series. From the atomic coordinates, corresponding to the ideal structural model (shown in Figure 3c), an image calculation has been performed in

the $P321$ space group. The best fit is obtained for $\Delta t = 7.0$ nm and $\Delta f = -65$ nm (Figure 3).

The HREM study of the (9:7), (14:11), and (21:17) compounds conclusively shows these phases are formed by the ordered intergrowth of the simplest members, $n = 2$ (TP:$2O_h$), $n = 3$ (TP:$3O_h$) and $n = 4$ (TP:$4O_h$), whose structure is directly related to n value. However, in the new materials, where $n = 2.5$ for the (9:7) phase (...TP:$2O_h$:TP:$3O_h$...), $n = 2.67$ for the (14:11) phase (...TP:$2O_h$:TP:$3O_h$:TP:$3O_h$...), and $n = 3.25$ for the (21:17) phase (...TP:$3O_h$:TP:$3O_h$:TP:$3O_h$:TP:$4O_h$...), the relationship between n and the structure is not so obvious because n corresponds to the average number of octahedra between prisms. A more instructive formula can be established from our knowledge of the structure of these compounds. For this purpose, we have considered that all materials are constituted by the ordered intergrowth of the smallest structural frames constituting the structures of the phases limiting this series: 2H-ABO_3 and $A_3B_2O_6$. As a consequence, the general expression including all members can be formulated as $(A_3B_2O_6)_\alpha$-$(A_3B_3O_9)_\beta$, with α and β denoting the number of each
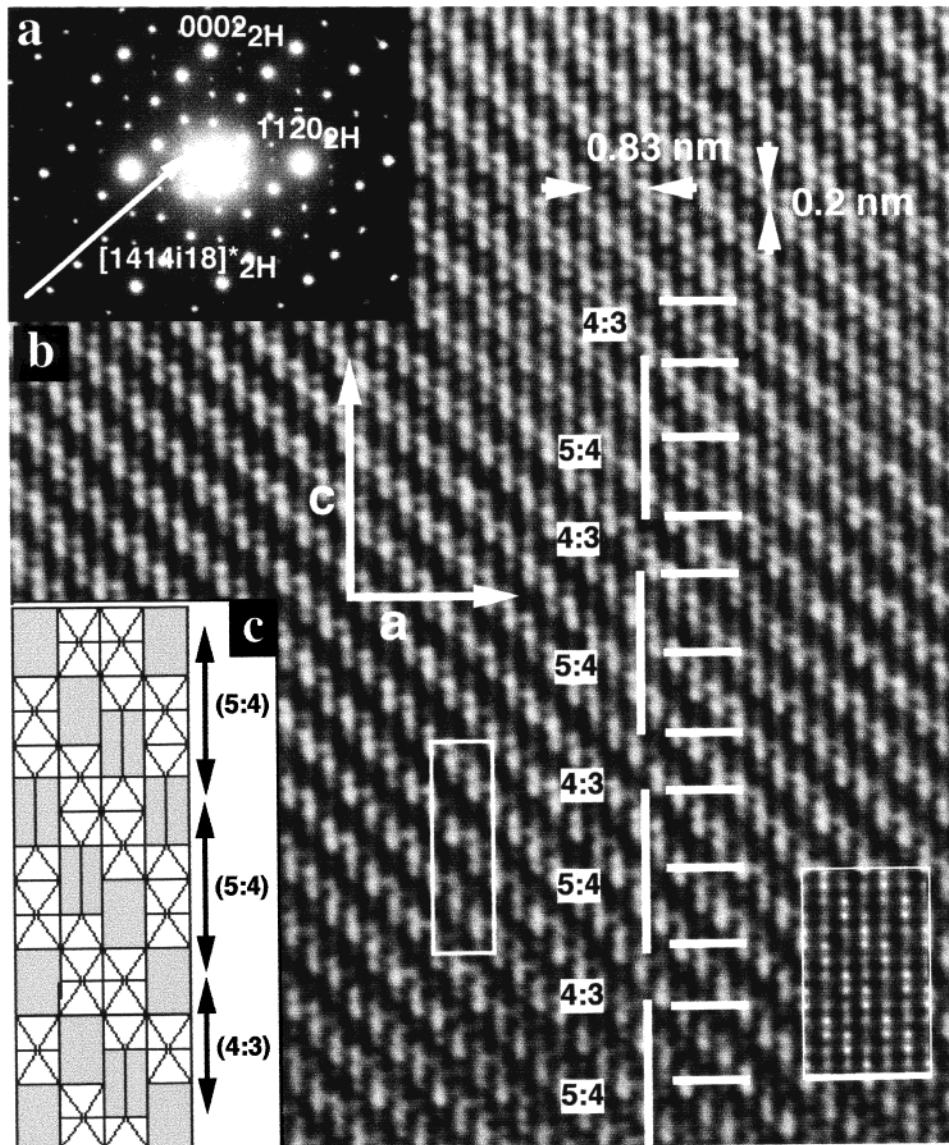
Figure 2. (a) SAED pattern along $[1\bar{1}00]_{2H}$ corresponding to $Sr_{14}Co_{11}O_{21}$. (b) Corresponding HREM image. The simulated image is shown at the inset. (c) Ideal structural model projected along $[1\bar{1}00]_{2H}$. It is formed by the ordered intergrowth of one (5:4) and one (4:3) unit cell, along c axis.

Table 1. Preparation Conditions and XRD Results for A−Co−O (A = Ca, Sr, Ba) Phases

A:Co	temp (°C)	time (days)	phase analysis (XRD)	a, c (nm)
9:7	800	5	$(Sr_{0.6}Ca_{0.4})_9Co_7O_{21}$ and (4:3) traces	0.93, 3.63
14:11	830	6	$Sr_{14}Co_{11}O_{33}$	0.94, 2.86
21:17	800	3	$Sr_{21}Co_{17}O_{51}$ and (5:4) traces	0.94, 8.49
15:13	940	3	$Ba_{15}Co_{13}O_{39}$	0.99, 6.52
10:9	900	60	$Ba_{66}Co_{59}O_{177}$	0.99, 14.52

block constituting every phase; α also refers to the number of prisms per unit cell, and $(3\alpha + 3\beta)$ is the number of layers, both A_3O_9 and $A_3A'O_6$, per unit cell. Therefore, the relationship between this formulation and the formalism $A_{n+2}A'B_nO_{3n+3}$ is that the latter is restricted to one prismatic site per unit formula whereas the former is more general, allowing α prismatic sites per formula.

All of the samples up to now isolated in the Sr−Ca−Co−O system are listed in Table 2. Notice that α is always $\geq \beta$. To stabilize phases with $\beta > \alpha$, the presence

of Ba in A positions is required.[6]

2. New Phases in the Ba−Co−O System. In this way, the ($\alpha = 6$, $\beta = 9$) member has been isolated according to the following relationship: $1Ba_7Co_6O_{18}$: $1Ba_8Co_7O_{21} = Ba_{15}Co_{13}O_{39}$. Figure 4 shows the SAED pattern and the corresponding HREM image along $[1\bar{1}00]_{2H}//[10\bar{1}0]_{15:13}$. Up to fourth-order satellites are seen along the modulation direction $[15\ 15\ i\ 12]^*_{2H}$. Once again, the diffraction spots can be considered as equispace sequences along such a direction. This is reflected in the HREM image (Figure 4b), which corresponds to an apparently well-ordered material whose structure can be described from the ordered intergrowth along the c axis of half of a unit cell of the (7:6) phase and one unit cell of the (8:7) member. Therefore, this material is constituted by 30 layers (18 Ba_3O_9 and 12 Ba_3CoO_6) with unit cell parameters $a = 0.99$ nm and $c = 6.52$ nm and trigonal symmetry. The ideal structural model is schematized in Figure 4c. The simulated image from the corresponding atomic coordinates, as well as $P321$ as space group, fits with the experimental one for
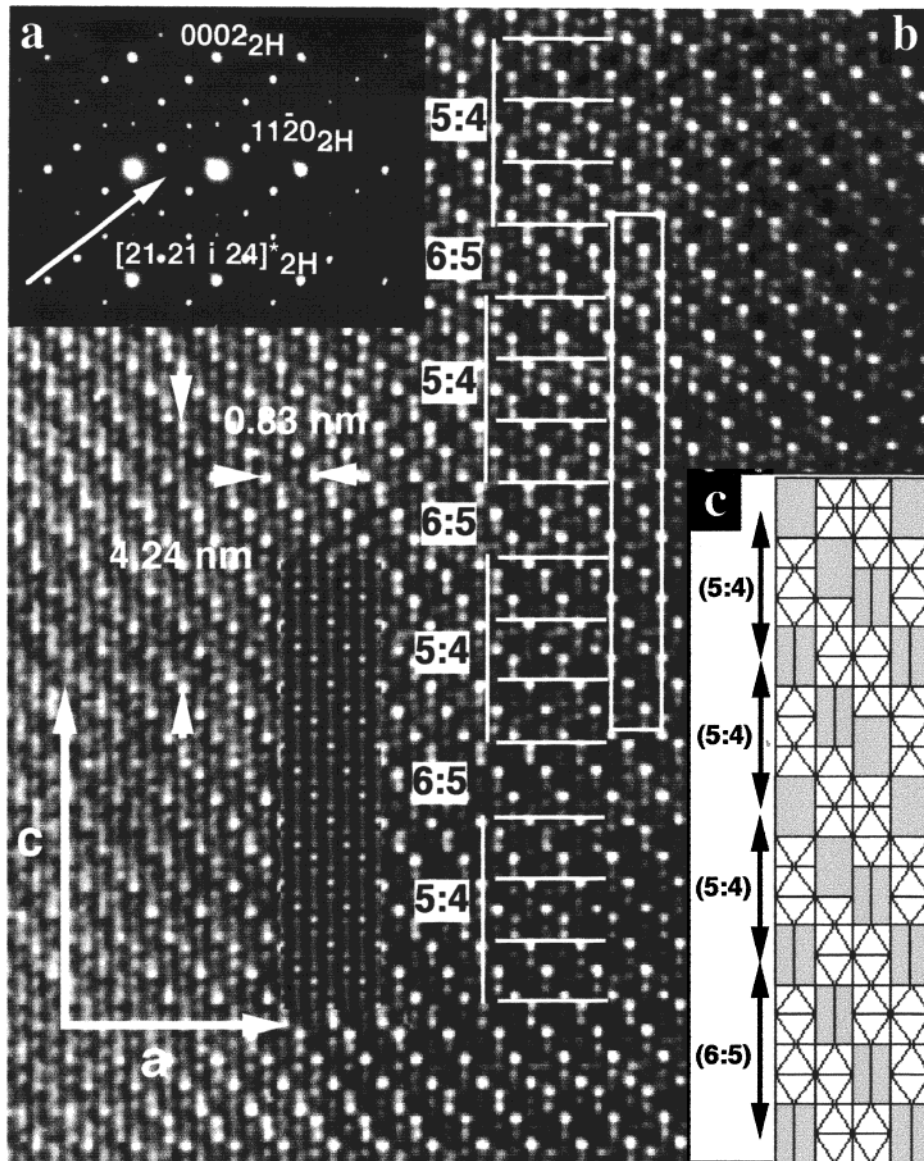
Figure 3. (a) SAED pattern along $[1\bar{1}00]_{2H}$ corresponding to $Sr_{21}Co_{17}O_{51}$. (b) Corresponding HREM image. The simulated image is shown at the inset. (c) Ideal structural model along $[1\bar{1}00]_{2H}$ (half of a unit cell is represented). Three blocks (5:4) and one block (6:5) constituting half of a unit cell of the (21:17) phase are marked.

Table 2. Chemical Composition, Structural Blocks and Crystallographic Data of (A₃Co₂O₆)ₐ(A₃Co₃O₉)ᵦ Phases

comp	α	β	$[\alpha + \beta\ \alpha + \beta i2\alpha]^*_{2H}$	$\mathbf{k} = (a^* + b^*)/3 + m2c^*_{2H}\ (m)$	$c_1/c_2 = 1 - m = \lambda$	ref
$Ca_3Co_2O_6$	3	0	[3.3 i 6]	1/3	2/3	4
$(Sr_{0.5}Ca_{0.5})_4Co_3O_9$	3	1	[4 4 i 6]	1/4	3/4	7
$(Sr_{0.5}Ca_{0.5})_9Co_7O_{21}$	2	1	[3 3 i 4]	2/9	7/9	a
$Sr_{14}Co_{11}O_{33}$	9	5	[14 14 i 18]	3/14	11/14	7,a
$Sr_5Co_4O_{12}$	3	2	[5 5 i 6]	1/5	4/5	7
$Sr_{21}Co_{17}O_{51}$	12	9	[21 21 i 24]	4/21	17/21	a
$Sr_6Co_5O_{15}$	3	3	[6 6 i 6]	1/6	5/6	17
$(Ba_{0.25}Sr_{0.75})_6Co_5O_{15}$	3	3	[6 6 i 6]	1/6	5/6	7
$(Ba_{0.5}Sr_{0.5})_7Co_6O_{18}$	3	4	[7 7 i 6]	1/7	6/7	6
$Ba_{15}Co_{13}O_{39}$	6	9	[15 15 i 12]	2/15	13/15	a
$Ba_8Co_7O_{21}$	3	5	[8 8 i 6]	1/8	7/8	6
$Ba_9Co_8O_{24}$	3	6	[9 9 i 6]	1/9	8/9	6
$Ca_{66}Co_{59}O_{177}$	21	45	[22 22 i 14]	7/66	59/66	a
$BaCoO_3$	0	1			1	5

a This work.

$\Delta t = 5$ nm and $\Delta f = -95$ nm (Figure 4).

$Ba_9Co_8O_{24}$ is the highest member up to now reported.[6] By using similar thermodynamic conditions, the hypothetical member, $Ba_{10}Co_9O_{27}$, has not been stabilized. The upper limit we have found for these synthesis conditions corresponds to the following relationship: $4Ba_9Co_8O_{24}:3Ba_{10}Co_9O_{27} = 1Ba_{66}Co_{59}O_{177}$. The structure of this phase can be built up from the ordered intergrowth of half of a unit cell of the $n = 7$ ($\alpha = 3$, $\beta = 6$) member, $Ba_9Co_8O_{24}$, and three blocks formed by half of
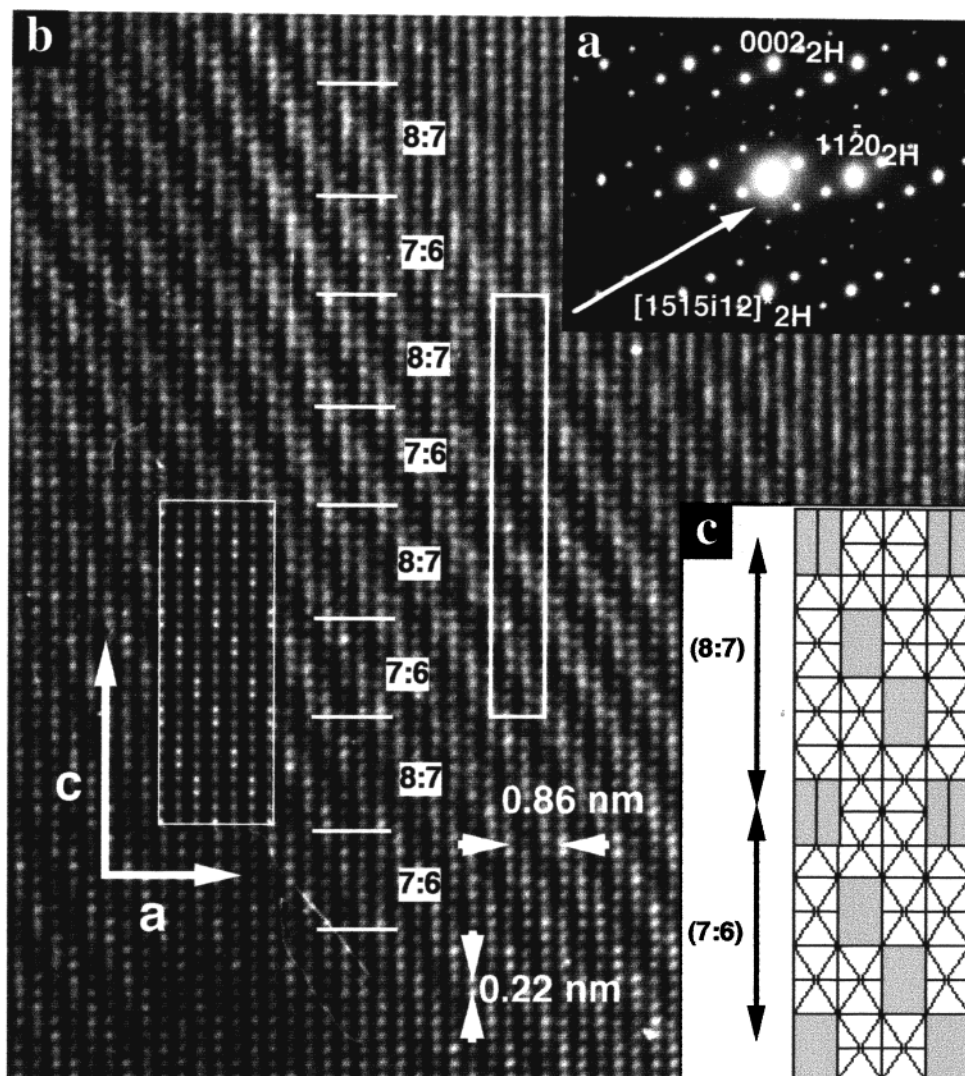
Figure 4. (a) SAED pattern along $[1\bar{1}00]_{2H}$ corresponding to $Ba_{15}Co_{13}O_{39}$. (b) Corresponding HREM image. The simulated image is shown at the inset. (c) Ideal structural model along $[1\bar{1}00]_{2H}$ (half of a unit cell is represented). Blocks (8:7) and (7:6) are marked.

a unit cell of the $n = 7$ and one unit cell of the $n = 8$, $Ba_{10}Co_9O_{27}$ ($\alpha = 3$, $\beta = 7$), as represented in Figure 5a. This situation corresponds to ($\alpha = 21$, $\beta = 45$) and is the upper limit of the series when Ba and Co occupy the metallic sublattice. The SAED pattern (Figure 5b) along the $[1\bar{1}00]_{2H}//[10\bar{1}0]_{66:59}$ zone axis shows the modulation direction which is, in this case, $[22\ 22\ i\ 14]^*_{2H}$. The HREM image (Figure 5c) shows again an apparently well-ordered material. Unit cell parameters are $a = 9.9$ nm and $c = 14.52$ nm, and the symmetry is trigonal. It is worth mentioning that although the stoichiometry of this compound is complex and the structural blocks constituting this phase are ordered in a complicated way, this kind of complex ordering is maintained along all of the crystal and in every crystal observed.

Discussion

The phases previously described constitute an example of superstructures formed by the juxtaposition of two structural types that are able to intergrow because both have an adaptable atomic arrangement along a given crystallographic plane. Such a behavior

has been shown by many structural types but is particularly frequent in perovskite-related materials. For instance, the ordered intergrowth between the cubic ABO_3 perovskite and the $A_2B_2O_5$ brownmillerite-type structure leads to the family of oxides corresponding to the $A_nB_nO_{3n-1}$ homologous series[14] formed by α (ABO_3) and β ($ABO_{2.5}$) structural blocks. This situation is analogous to that found in the monodimensional hexagonal perovskite-related compounds because, from the HREM results, all of the phases stabilized in the A−Co−O system can be considered as formed by the ordered intergrowth of 2H-ABO_3 and $A_3B_2O_6$ and constituting the $(A_3B_2O_6)_\alpha(A_3B_3O_9)_\beta$ series. These phases present the same structural features, and they can be considered as modulated superstructures of the 2H-type. Effectively, modulated structures are observed in all cases, but all reflections appearing in the SAED patterns, even those which can apparently be considered as satellites, can be indexed on the basis of conventional three-dimensional lattices, thus confirming that all these structures are commensurable. As a consequence,

(14) Grenier, J. C.; Darriet, J.; Pouchard, M.; Hagenmuller, P. *Mater. Res. Bull.* **1976**, *11*, 1219.
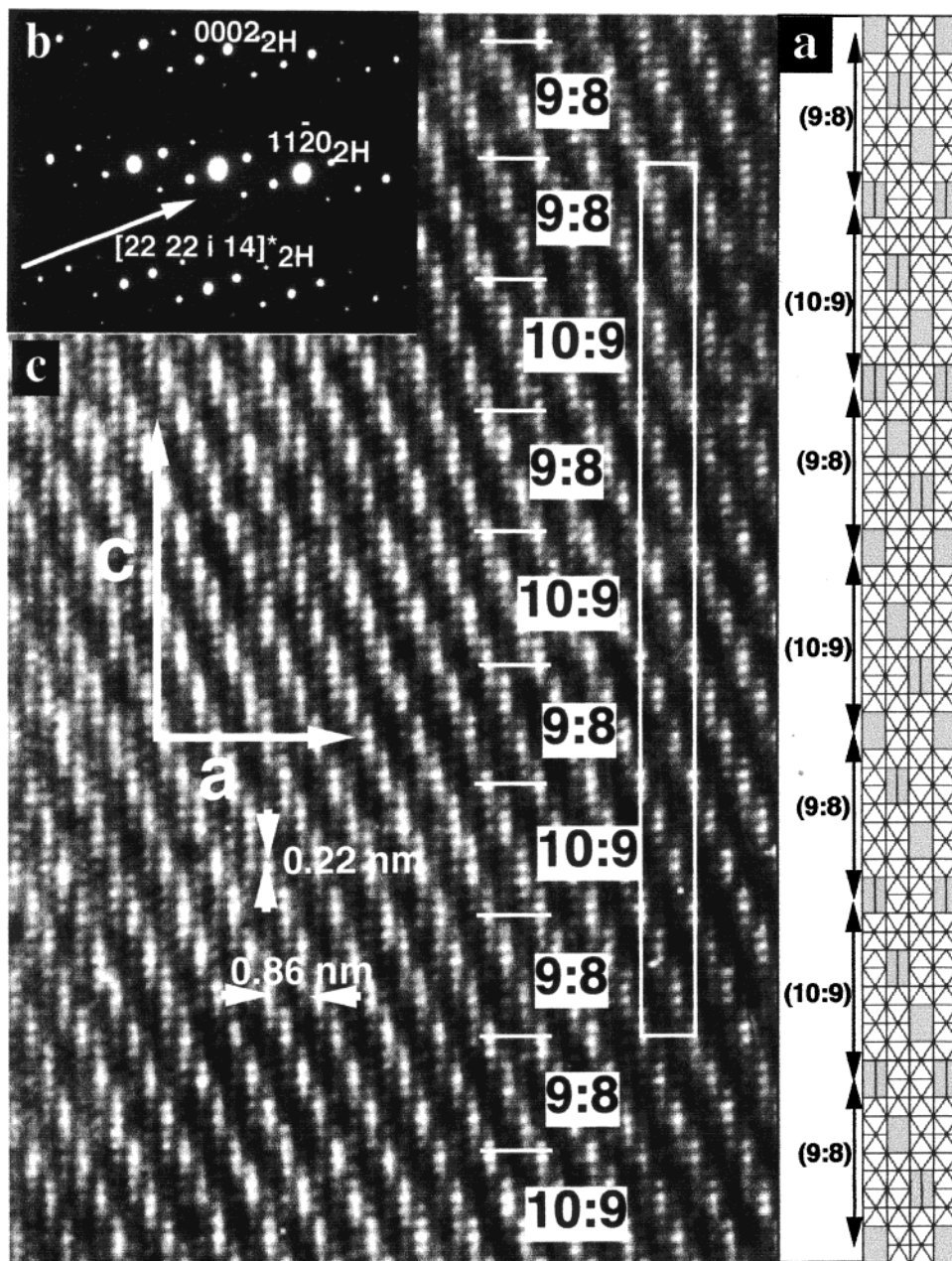
Figure 5. (a) Ideal structural model corresponding to $Ba_{66}Co_{59}O_{177}$, along $[1\bar{1}00]_{2H}$ (half of a unit cell is represented). (b) SAED pattern and (c) HREM image along $[1\bar{1}00]_{2H}$.

they can be described from the 2H basic unit cell with the modulation given by a vector **k**, determined from the $[1\bar{1}00]_{2H}$ zone, which can be expressed as $\mathbf{k} = (a^*_{2H} + b^*_{2H})/3 + m2c^*_{2H}$, with m being a rational fraction. m also reflects the α $(A_3B_2O_6)$ blocks intergrowing with β $(A_3B_3O_9)$ blocks according to the expression: $m = \alpha/3\alpha + 3\beta$, with $[\alpha + \beta\alpha + \beta i2\alpha]^*_{2H}$ being the 2H superstructure direction.

All of the members isolated in the A–Co–O system are gathered in Table 2, including the α and β values for every one and the modulation vector that describes these commensurable phases. Note that by assuming the II oxidation state for both A cations and B cations prismatically coordinated and the IV oxidation state for B cations octahedrally coordinated, the charge balance is achieved whatever the α and β values. The chemical analysis only gives an average Co oxidation state, which, in all cases, fits with a ratio Co^{II}(prismatic sites)/Co^{IV}-

(octahedral sites), i.e., corresponding to $\alpha/(\alpha + 3\beta)$, according to the larger atom in trigonal prismatic coordination. This distribution may represent a charge-ordering situation between Co^{IV} and Co^{II} as proposed for $Ca_3Co_2O_6$.[4] Susceptibility measurements versus temperature shows paramagnetic behavior between 4 and 295 K following a Curie–Weiss law, in all materials. However, this preliminary study is not enough to distinguish the oxidation state of Co atoms, because the effective magnetic moment is always lower than that estimated for any theoretical calculation without considering both orbital contribution and specific magnetic structure, suggesting that strong magnetic interactions can exist in these compounds even at room temperature. To understand this complex magnetic behavior, neutron diffraction studies of the (14:11) sample are in progress.

As a summary, Figure 6 represents, in a schematic way, the $[1\bar{1}00]_{2H}$ reciprocal plane showing the variation
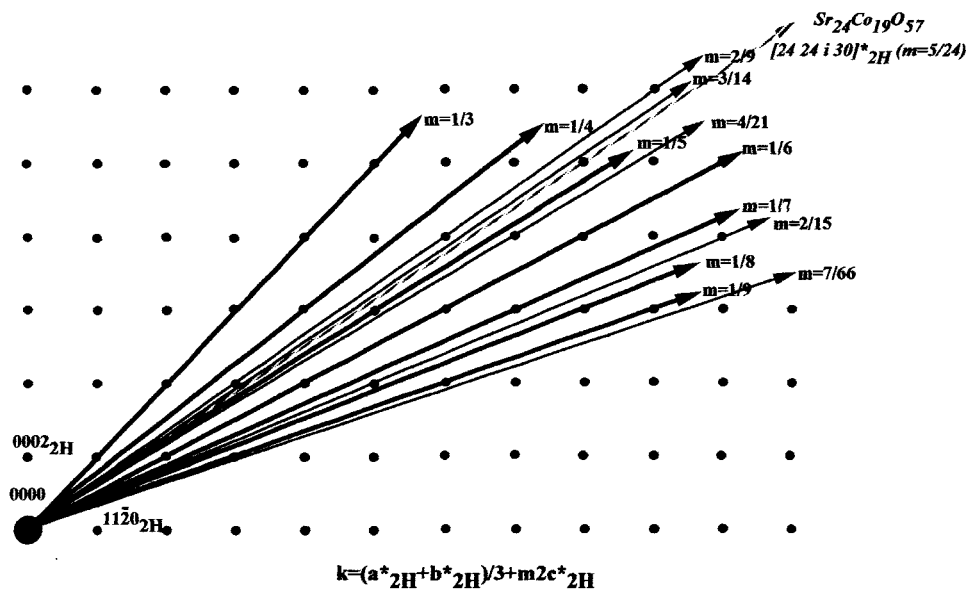
Figure 6. Schematic representation of the $[1\bar{1}00]_{2H}$ reciprocal plane showing the variation of vector **k** as a function of the A/Co ratio. The coarse black arrows refer to *n* integer and fine black arrows to *n* nonintegral members of the $A_{n+2}CoCo_nO_{3n+3}$ homologous series. The 2H superstructure direction and the *m* value for $Sr_{24}Co_{19}O_{57}$ [10,15] are also included.

of vector **k** as a function of the composition of the different members isolated in the A−Co−O system. By starting from the 2H−BaCoO₃ phase ($m = 0$, $\alpha = 0$, $\beta = \infty$), and keeping A = Ba the same, it is possible to stabilize phases with $0 \le m \le 0.133$. In all cases, $\alpha < \beta$; i.e., these are the phases with the lowest ratio TP/O$_h$. To increase the *m* value (the ratio TP/O$_h$ per unit cell), it is necessary to decrease the average size of the A cation. The partial substitution of Ba by Sr stabilizes phases with higher α/β ratios. Thus, for $(Ba_{0.25}Sr_{0.75})_6$-Co₅O₁₅, α becomes equal to β. When Sr fully occupies the A sites, phases with $\alpha \ge \beta$ can be isolated. The partial substitution of Sr by Ca is accompanied of an increasing of *m*, i.e., an increasing of the α/β ratio, up to Ca₃Co₂O₆ where $m = {}^2/_3$ and $\alpha = \infty$ ($\beta = 0$).

By changing the substituents in the A sublattice, and keeping B=Co the same, a lot of phases between the lower limit (Ca₃Co₂O₆) and Ba₆₆Co₅₉O₁₇₇ have been stabilized. As it can be seen, between this one and BaCoO₃, none of the members has been isolated. By considering that 2H− BaCoO₃ can only be stabilized under high-pressure conditions, it is possible that to be isolated members with $0 \le m < {}^7/_{66}$ require higher pressures than that of the atmospheric conditions.

Obviously, other combinations, different from those gathered in Table 2, between α and β can be envisaged, leading to new, different compositions of commensurate modulated phases. For instance, the phase $Sr_{24}Co_{19}O_{57}$, as announced by Evain et al.,[10] will be reported by Gourdon et al.[15] According to this composition, its structure could be formed by 15 (Sr₃Co₂O₆) and 9 (Sr₃-Co₃O₉) structural frames. The modulation direction should correspond to $[24\ 24\ i\ 30]^*_{2H}$, between $[55\bar{6}]^*_{2H}$, corresponding to the 5:4 phase, and the $[44\bar{8}6]^*_{2H}$ corresponding to the (4:3) phase, as foreseeable because two (5:4) and one (4:3) unit cells intergrowing in an

ordered way must constitute this phase. As it can be seen, from a structural point of view, different phases can be stabilized for any α and β values thus leading to the so-called *composition flexible structures*.[16]

As a final comment, we mention that alternatively, as it has been previously shown by Ukei et al.,[9] the SAED patterns could be indexed using the composite crystal model considering the structures as formed by two subsystems with the same unit cell parameters *a* and *b* ($a^* = b^* = a^*_{2H}/3$) but with different c^*_1 and c^*_2 parameters. c^*_1 is the separation between equivalent AO₃ layers and, therefore, is referred to c^*_{2H}; c^*_2 is the mean spacing of the cations within the polyhedra chains. It is very easy to change from one to another notation if one consider that $m2c^*_{2H} = c^*_1 − c^*_2$ and then $c^*_2/c^*_1 = (1 − m)$. According to Evain et al.,[10] in the case of a commensurate composite structure, $c_1 = \gamma c_2$, γ, and so on $(1 − m)$, can be expressed as a rational fraction. This is the case of all materials reported in this paper (see Table 2). These results show that many structures of hexagonal perovskite-type compounds can be adequately characterized, even when single crystals are not available, from the information given by the combination of SAED and HREM. However, due to the limitation in accurate placement of light atoms using SAED and HREM, small deviations from the commensurate models as those related with the intermediate character between ideal octahedra and trigonal prisms cannot be detected.

(15) Gourdon, O.; Boucher, F.; Petricek, V.; Evain, M. *Acta Crystallogr. B.*, in press.

(16) Withers, R. L.; Schmid, S.; Thompson, J. G. *Prog. Solid State Chem.* **1998**, *26*, 1.
(17) Harrison, W. T. A.; Hegwood, S. L.; Jacobson, A. J. *J. Chem. Soc., Chem. Commun.* **1995**, 1953.